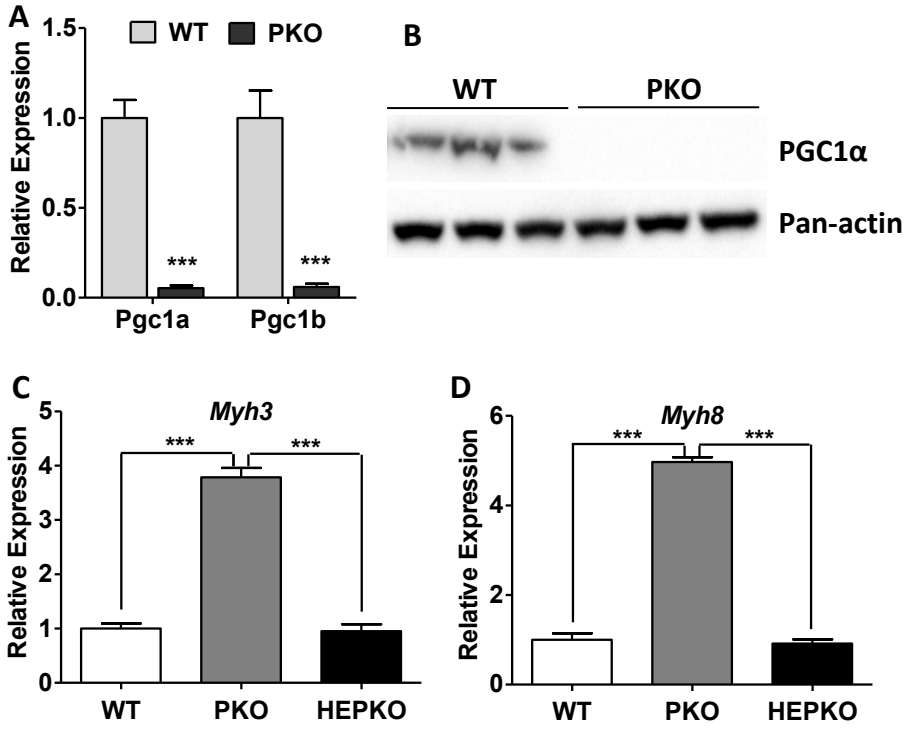

Figure S1 (related to Fig. 1). ERRγ improves running defect and muscle damage in PGC1-null mice. (A) Relative RNA expression levels of *Pgc1a* and *Pgc1b* in WT vs PKO plantaris; (B) Western blot showing Pgc1a and actin protein levels in WT vs PKO soleus; (C-D) Relative RNA expression levels of *Myh3* (C) and *Myh8* (D) in plantaris. (n=5, ***p < 0.001)

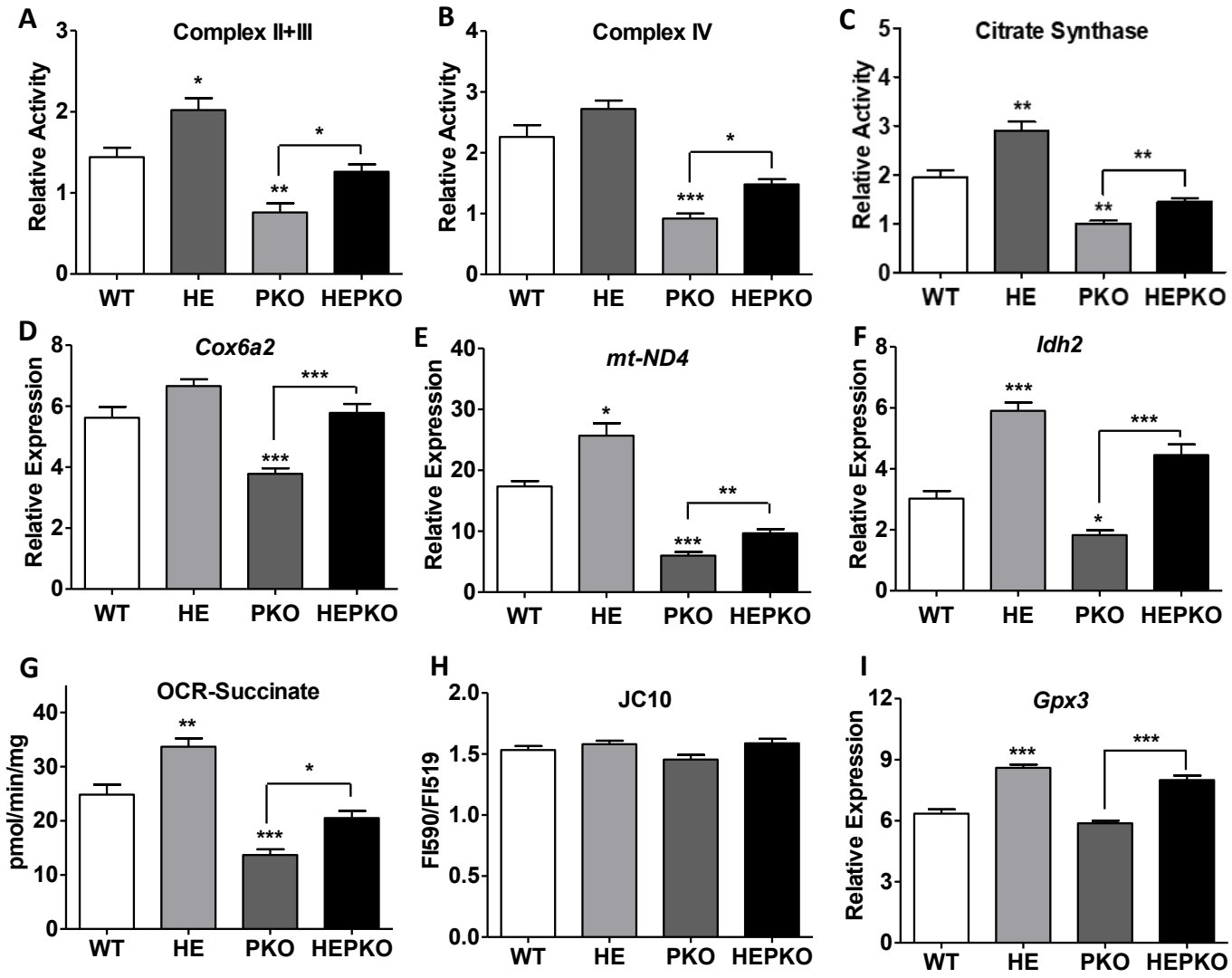

Figure S2 (related to Fig. 2). ERRγ improves mitochondrial energetic defects in PGC1-null muscle. (A-C) mitochondrial complex II+III activity (A), complex IV activity (B), and citrate synthase activity (C) measured in isolated mitochondrial from quadriceps muscle; (D-F) RNA expression levels of *Cox6a2* (D), *mt-Nd4* (E), and *Idh2* (F) in plantaris; (G) oxygen consumption rate measured in freshly isolated quadriceps mitochondria using succinate as substrate; (H) mitochondrial membrane potential measured as JC-10 fluorescence intensity ratio at 590nm/519nm in freshly isolated quadriceps mitochondria; and (I) RNA expression of *Gpx3* in plantaris. (n=5; *p < 0.05, **p < 0.01, ***p < 0.001)

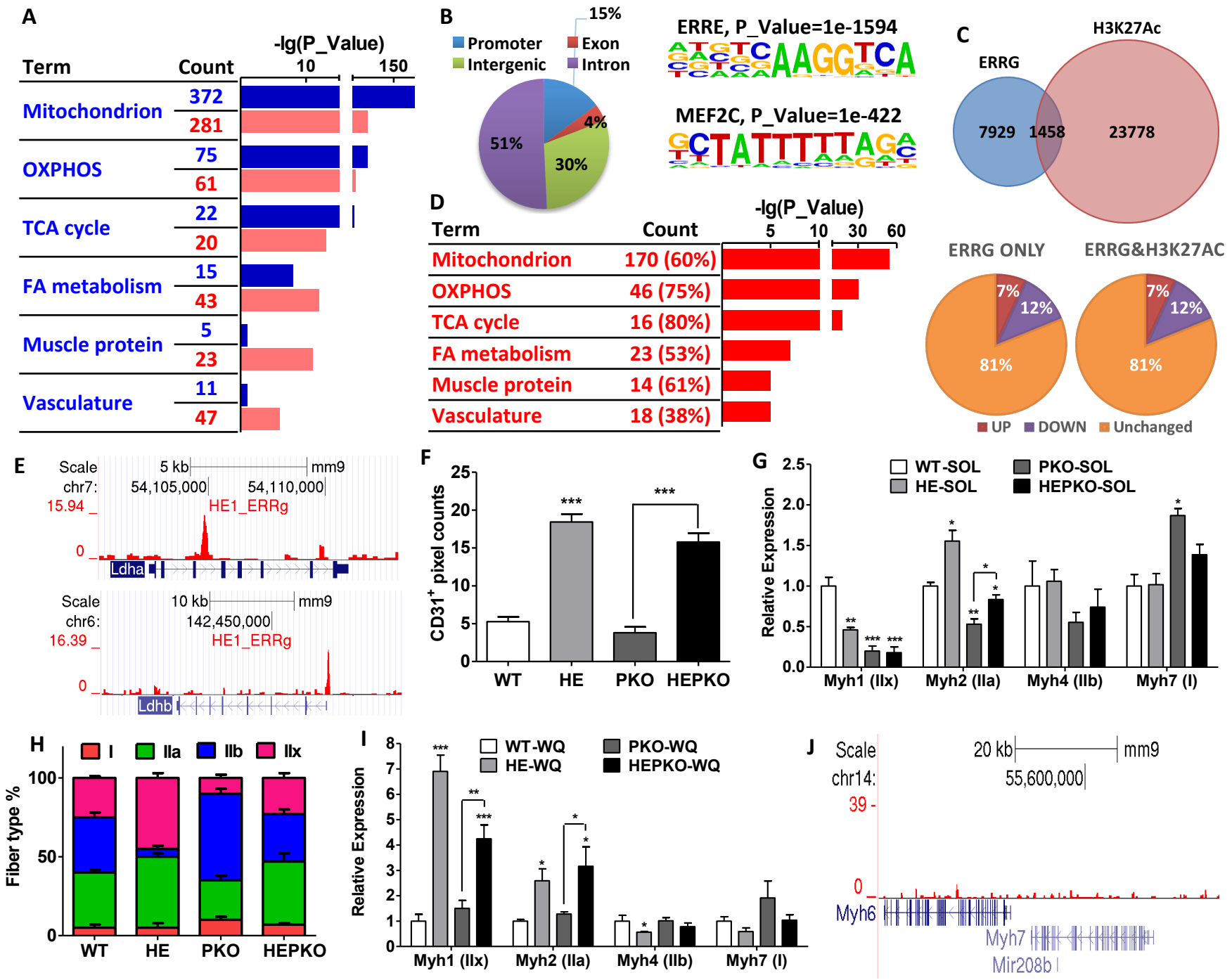

Figure S3 (related to Fig. 3). ERRγ induces oxidative muscle remodeling in the absence of PGC1. (A) Gene ontology analyses of down-regulated (blue) genes in PKO vs WT SOL and up-regulated (red) genes in HE vs WT WQ muscle; (B) schematic showing genomic distribution of ERRγ-bound peaks (left) and a consensus ERRE and a MEF2c motif that are highly enriched in the ERRγ-bound regions (right); (C) ERRγ- and H3K27Ac-bound sites and sites co-occupied by both factors shown in Venn diagram (top), and the percentages of genes upregulated (purple), downregulated (blue), or unchanged (brown) by ERRγ overexpression that contain ERRγ binding sites or ERRγ/H3K27Ac co-occupied sites (bottom); (D) gene ontology analyses of ERRγ-bound and up-regulated genes in HE vs WT WQ muscle, with their percentages of total ERRγ-induced genes in parentheses; (E) genome browser tracks showing ERRγ binding at *Ldha* and *Ldhb*; (F) quantitative pixel counts in CD31 immunostaining (mean counts from 5 fields per section); (G) RNA expression of Myh1/2/4/7 in SOL; (H) quantitative fiber-typing analysis from Myh-immunostaining in Fig. 3D; (I) RNA expression of Myh1/2/4/7 in WQ; and (J) genome browser track showing no ERRγ binding at the slow-twitch *Myh7* gene. (n=5; *p < 0.05, **p < 0.01, ***p < 0.001)

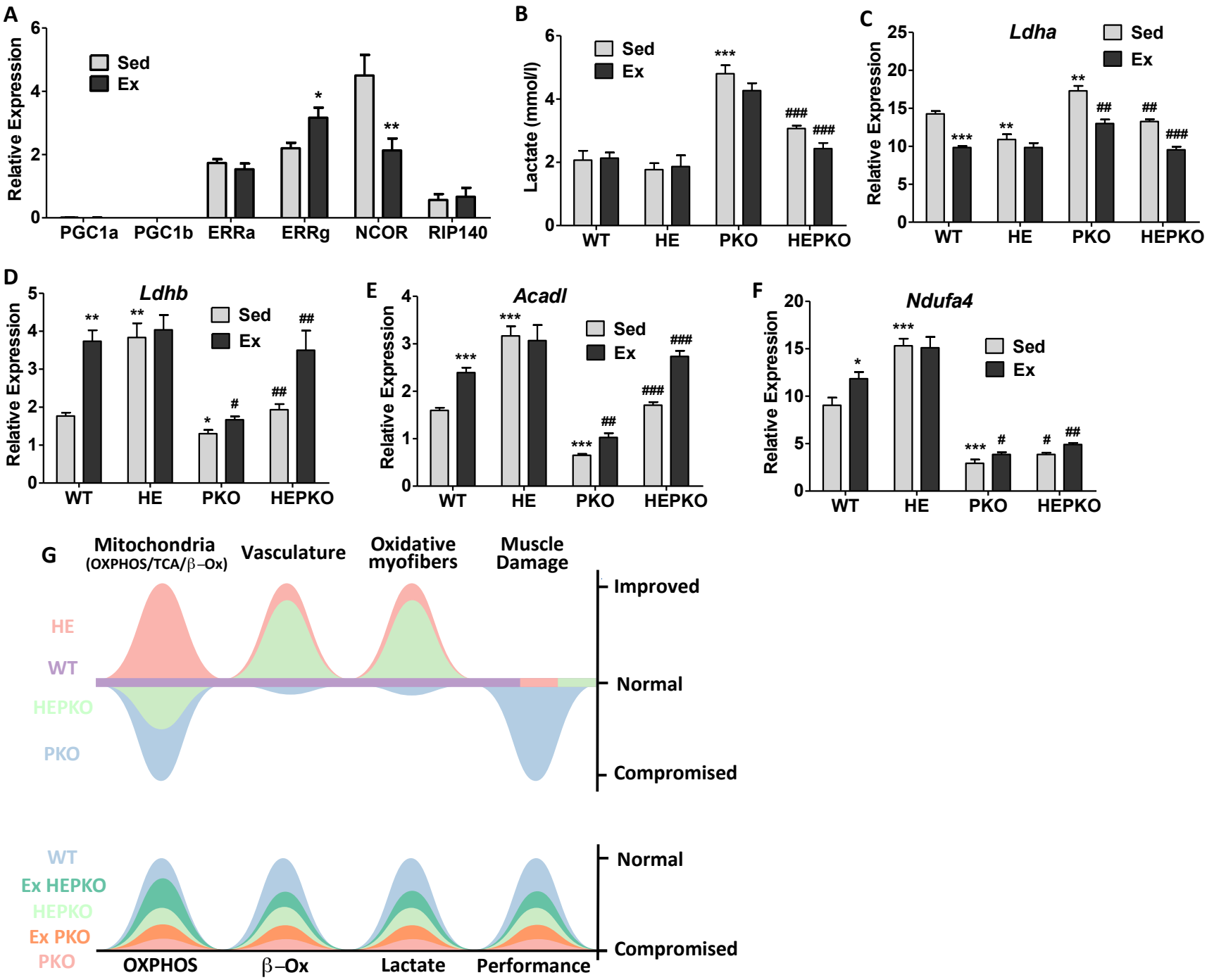

Figure S4 (related to Fig. 4). Exercise and ERRγ synergistically improve oxidative functions in PKO muscle. (A) RNA expression levels of PGC1a/b, ERRa/g, NCOR, and RIP140 in PL muscle from sedentary vs exercised PKO mice; (B) Blood lactate level after 7 minutes of endurance running (when the first mouse failed); (C-F) RNA expression levels of *Ldha* (C), *Ldhb* (D), *Acadl* (E), and *Ndufa4* (F) in plantaris; and (G) schematic showing phenotypic changes in genetic models and combinational benefits of both ERRγ gain of function and voluntary exercise in PKO mice. (n=5; * and # show statistical difference from WT and PKO, respectively. * and # $p < 0.05$, ** and ## $p < 0.01$, *** and ### $p < 0.001$)